OPEN

Effects of electroacupuncture on neural function and the expression of inflammation-related proteins NLRP3/caspase-1 in rats with ischemic stroke

Zhifeng Wang[a,*], Yujiang Xi[a,*], Junfeng Lan[a,*], Jiao Yang[b], Ting Shi[a], Shuangfeng Xu[a], Liwei Xing[a], Pan Pan[b] and Jian Wang[a]

This study aimed to investigate the neuroprotective effects of electroacupuncture (EA) at the Baihui and Dazhui acupoints in a rat model of ischemia-reperfusion injury. Ninety-six male Sprague–Dawley rats were randomly assigned to four groups ($n = 24$ per group): Sham, middle cerebral artery occlusion (MCAO), MCAO+EA, and MCAO+MCC950. The MCAO model was induced using filament embolization. Neurological function was assessed using Zea Longa scores on days 1 and 7 posttreatment, while cerebral infarction volume was measured using 2,3,5-triphenyltetrazolium chloride staining. Gene expression levels of NLRP3 and GSDMD were quantified by RT-qPCR, and protein expressions of NLRP3, GSDMD, caspase-1, IL-1β, and IL-18 were evaluated via Western blotting, immunohistochemistry, immunofluorescence staining, and ELISA. On day 1, compared with the MCAO group, the MCAO+EA and MCAO+MCC950 groups exhibited significantly reduced mRNA and protein expressions of NLRP3 and GSDMD ($P < 0.05$), as well as decreased levels of caspase-1, IL-1β, and IL-18 ($P < 0.05$). However, no significant differences were observed in neurological deficit scores or cerebral infarction volume. By day 7, both the MCAO+EA and MCAO+MCC950 groups showed significant improvements in neurological function ($P < 0.05$), reductions in cerebral infarction volume ($P < 0.05$), and further decreases in the expression of NLRP3, GSDMD, caspase-1, IL-1β, and IL-18 ($P < 0.05$). EA at the Baihui and Dazhui acupoints alleviates neurological deficits in ischemic stroke rats by inhibiting the NLRP3/caspase-1 inflammatory pathway and reducing the expression of apoptosis-related proteins such as NLRP3, GSDMD, caspase-1, IL-1β, and IL-18. *NeuroReport* 36: 456–466 Copyright © 2025 The Author(s). Published by Wolters Kluwer Health, Inc.

NeuroReport 2025, **36**:456–466

Keywords: caspase-1, electroacupuncture, ischemic stroke, neuroinflammation, NOD-like receptor protein 3

[a]The First Clinical Medical College, Yunnan University of Chinese Medicine, Kunming, China and [b]College of Acupuncture and Massage, Yunnan University of Chinese Medicine, Kunming, China

Correspondence to Jian Wang, MD, The First Clinical Medical College, Yunnan University of Chinese Medicine, No. 1076, Yuhua Road, Chenggong District, Kunming City, Yunnan Province, China
Tel: +86 15812111635; e-mail: laohaodiao@126.com

*Zhifeng Wang, Yujiang Xi, and Junfeng Lan contributed equally to this work and share the first authorship.

Received 4 February 2025 **Accepted** 4 April 2025.

Introduction

Ischemic stroke is a potentially fatal cerebrovascular disease, defined as a sudden decrease in blood supply to a specific brain region. Approximately 14 million people worldwide suffer from stroke each year. It is the leading cause of permanent disability and the second leading cause of global mortality [1]. Many ischemic cascades occur after ischemic stroke, and neuroinflammatory injury plays an important role in the injury process. An increasing number of studies have shown that anti-inflammatory therapy may serve as a novel treatment option for ischemic stroke. The neuroinflammatory response after stroke is a cascade amplification process. From a few minutes to a few hours after cerebral ischemia, the interruption of blood flow allows the damaged tissue to rapidly release proinflammatory mediators such as reactive oxygen species (ROS) from the damaged tissue, which not only activates the intracranial microglia, but also induces the expression of brain endothelial cells and peripheral white blood cell surface adhesion molecules, thereby promoting the infiltration of peripheral white blood cells into the cerebral ischemic area. In the hours to days after a stroke, more nitric oxide and ROS are generated, activating metal matrix protease, which causes the cascade amplification of the neuroinflammatory response, ultimately leading to the destruction of the blood-brain barrier, brain edema, and neuronal cell death [2].

Inflammasomes are an important part of the endogenous immune response in ischemic stroke. Activation of the NOD-like receptor protein 3 (NLRP3) inflammasome is primarily observed in microglia and contributes to the secretion of proinflammatory cytokines and subsequent inflammatory responses in the pathological process

of ischemic stroke. Brain ischemia leads to increased expression of the components of the NLRP3 inflammasome pathway, including NLRP3, apoptosis-associated speck-like protein containing a caspase recruitment domain (ASC), procaspase-1, pro-IL-1β, and pro-IL-18 in the neurons and ischemic brain tissues. The levels of caspase-1, IL-1β, and IL-18 and the products of the activated NLRP3 inflammasome are increased, and caspase-1, IL-1β, and IL-18 are present in the cytoplasm of neurons, indicating enhanced expression and activation of the NLRP3 inflammasome in cerebral ischemia. The activated NLRP3 inflammasome recruits and activates the precursor of caspase-1 through ASC, transforming it into active caspase-1. Activated caspase-1 further exerts its function, cleaves, and activates inflammatory factors such as IL-1β and IL-18 [3]. These inflammatory factors are then released into the extracellular environment, where they bind to the corresponding receptors and trigger a strong inflammatory response, thus aggravating nerve inflammation and injury. The application of caspase-1 inhibitors can reduce the levels of caspase-1, IL-1β, and IL-18 and can reduce neuronal injury, the ischemic reperfusion brain tissue infarct area and neurological function injury in vitro models [4]. There is also evidence that NLRP3 inflammasome inhibitors mainly inhibit the activation of the NLRP3 inflammasome by targeting NLRP3 and ASC, which can reduce cerebral ischemia injury and inhibit nerve cell necrosis [5]. The above evidence indicates that the NLRP3 inflammasome may mediate cerebral ischemic injury and play an important role in the pathological mechanism of cerebral ischemia. Consequently, the NLRP3 inflammasome may be an important potential target for intervention in cerebral ischemia [6].

Electroacupuncture (EA) is a treatment modality that integrates traditional acupuncture with electrotherapy, and it is capable of reducing secondary neuronal death in the ischemic penumbra. It has significant effects on reducing the severity of ischemic stroke, improving neurological function, and reducing sequelae, but its mechanism of action remains unclear. Studies have shown that EA treatment can relieve neuroinflammation by inhibiting the miR-223/NLRP3 pathway, thus exerting neuroprotective effects on rats with middle cerebral artery occlusion (MCAO) [7]. This finding suggested that the neuroprotective mechanism of EA in MCAO rats may be related to the regulation of the NLRP3 pathway. Our study is based on this research and further investigates the mechanism through which EA regulates pyroptosis-related proteins to mitigate neural injury in ischemic stroke. NLRP3 plays a crucial role in coordinating host physiology and shaping central and peripheral immune/inflammatory responses by releasing IL-18 and IL-1β [8]. After ischemic stroke, a series of events called the 'ischemic cascade' increases the levels of proinflammatory mediators, including IL-18 and IL-1β, which damage healthy neurons and aggravate the initial ischemic injury. Therefore, we speculated that EA likely achieves its neuroprotective effects by regulating the NLRP3/caspase-1 pathway and reducing the expression of IL-18 and IL-1β inflammatory factors and cell pyroptosis-related proteins. This study aimed to explore the potential mechanism of EA in reducing nerve injury in ischemic stroke through the NLRP3/caspase-1 inflammatory pathway.

Materials and methods

Animals

120 male Sprague–Dawley rats (weight: 220 ± 10 g) were provided by the Experimental Animal Center of Kunming Medical University [license number: SCXK(Dian) K2020-0015]. They were housed in a controlled environment with a temperature of 23.2 °C, humidity of 60%, and a 12-h light-dark cycle. The rats were provided with standard feed and had free access to food and water. The 120 rats were randomly divided into four groups, with 30 rats in each group: sham surgery group, MCAO group, MCAO+EA group, and MCAO+MCC950 group. The MCAO group, the MCAO+EA group, and the MCAO+MCC950 group were subjected to the preparation of the MCAO model, while the Sham group only underwent the separation of the left common carotid artery (CCA). After subsequent MCAO modeling and experimental intervention, some rats died, leaving 24 rats in each group, a total of 96 rats. The animal experiments in this study were conducted in accordance with the 2006 Guidelines for Laboratory Animal Welfare and Use issued by the Ministry of Science and Technology of China.

Reagents and instruments

The reagents and instruments used in this research included a digital medical image analysis system (MOTIC Asia Optical Technology Co. Ltd., China); EA equipment (HANS-200A, Jisheng Medical instrument Co., Ltd., China); stainless steel disposable acupuncture needles (Hwato, 0.18 × 13 mm, Suzhou Medical Equipment Factory, China); Bicinchoninic acid (BCA) protein quantification test kit (Beyotime Institute of Biotechnology, China); primary antibody diluent for Western blotting (GTX28208) (Beyotime Institute of Biotechnology, China); NLRP3 antibody (TA336883) (Beijing Zhongshan Jinqiao Company, China, mouse-derived antibody, 1:1000), interleukin-1β antibody (TA506440) (Beijing Zhongshan Jinqiao Company, China, mouse-derived antibody, 1:4000), interleukin-18 antibody (10663-1-AP) (Wuhan Sanying Biotechnology Co., Ltd., China, rabbit-derived antibody, 1:2000), caspase-1 antibody (TA336409) (Beijing Zhongshan Jinqiao Company, China, mouse-derived antibody, 1:1000), GSDMD antibody (20770-1-AP) (Wuhan Sanying Biotechnology Co., Ltd., China, rabbit-derived antibody, 1:2000); β-actin antibody (20536-1-AP) (Wuhan Sanying Biotechnology

Co., Ltd., China, rabbit-derived antibody, 1:4000); goat antimouse IgG H&L (Alexa Fluor488) (ab150113) (Abcam, China, 1:5000); goat antirabbit IgG H&L (Alexa Fluor647) (ab150079) (Abcam, China, 1:5000); antimouse IgG (H + L) Antibody (5220-0341) (Seracare, China, 1:5000); antirabbit IgG (H + L) antibody (5450-0010) (Seracare, China, 1:5000); ammonium persulfate (MYM Biological Technology Co. Ltd., USA); polyvinylidene fluoride membrane (Invitrogen Reagent Corporation, Carlsbad, USA); IL-1β, IL-18 ELISA Research Kit (Jiangsu Meimian industria Co. Ltd, Jiang Su, China); and reagents for glycine, 56-40-6 (Biosharp Biotechnology life science Co. Ltd., China); 30% acrylamide and BIO-BEST 300 M gel imaging analysis system (Solarbio Science and Biotechnology Co., Ltd., China); Ultra High Sensitivity ECL chemiluminescence kit, batch number: 50018 (Beyotime Institute of Biotechnology, China); and MCC950 powder and DMSO (MedChemExpress LLC, China).

Ischemic stroke model

For the MCAO, MCAO+EA, and MCAO+MCC950 groups, an ischemic stroke model was established following previously described methods [9]. Briefly, anesthesia was induced via intraperitoneal administration of 3.5% pentobarbital sodium. A midline cervical incision was made, and the underlying tissues were carefully dissected layer by layer to expose and isolate the external carotid artery (ECA), internal carotid artery (ICA), and left CCA. The ECA and its branches were ligated and separated. A small incision was made at the proximal end of the ECA, through which a silicone-coated monofilament was inserted into the intracranial segment of the ICA. The filament was advanced to a depth of approximately 18 ± 0.5 mm from the carotid bifurcation to occlude blood flow to the middle cerebral artery (MCA). After confirming proper placement, the filament was withdrawn after 90 min to restore blood flow. Postoperatively, animals were monitored for any abnormalities, and their skin incisions were closed with sutures. They were returned to their cages with thermal insulation and regular monitoring. Animals exhibiting intact neurological function or those that died within the observation period were excluded from further analysis. In the sham-operated group, only the left CCA was isolated without further intervention. No thrombus or hemorrhage was observed in the ICA, confirming successful reperfusion.

Intervention methods

In the MCAO+EA group, after modeling, an EA intervention was performed on day 1. Acupoint selection was performed according to 'Development of Rat Acupoint Sites' [7]. 'Baihui (GV20)' (the middle of the parietal bone of rats) and 'Daizhui (GV14)' (the depression of the subspinal process of the seventh cervical spine in the prone position on the posterior midline) were selected. Acupuncture at the GV20 was performed by oblique insertion to a depth of 2 mm along the scalp midline toward the forehead. At the GV14, the needle was inserted perpendicularly to a depth of 5 mm. Following needle insertion, EA stimulation was delivered simultaneously to both acupoints using a Hans-200 EA instrument set at a frequency of 2 Hz/10 Hz and an intensity of 1 mA to generate the density wave [10]. Identical waveform parameters were applied to both GV20 and GV14 acupoints. The needles were retained for 30 min during the stimulation protocol. EA treatment was delivered on a daily basis for a consecutive 7-day period [7,11]. To avoid discomfort to the rats, the entire procedure was conducted swiftly, gently, and without interruption. Before the use of EA, conscious rats were trained for 2 weeks to acclimatize them to the manipulation and EA procedures [12]. Twice a week, the rat's body (including the limbs and head) was gently immobilized in a sling for 30 min. This method safely and effectively immobilized the rats. Acupuncture needles (0.18 mm) were inserted into and left in the muscles of the rat's head for 30 min during the restraint procedure to allow the rat to adapt to EA needling. Based on the observation that the rats were sufficiently acclimatized to the needling procedure by days 13 to 14, a 2-week training period was selected for the rats. In the MCAO+MCC950 group, intervention was also initiated on the first day after modeling. The intervention method involved intraperitoneal injection of MCC950 (3 mg/kg) [13]. The MCC950 solution was prepared by dissolving the MCC950 powder in DMSO, followed by the addition of sterile saline in a 1:1 ratio. Rats were then administered an intraperitoneal injection once daily for 7 days. The MCAO+MCC950 group was immobilized for the same duration each day as the MCAO + EA group. MCC950 serves as an inhibitor of NLRP3. The purpose of its utilization is to inhibit the activation of NLRP3 inflammasomes and mitigate the initiation of inflammatory cascades, allowing for comparison with the EA group and other control groups. The Sham group and the MCAO group were not subjected to any intervention, but they were immobilized for the same duration of time as the MCAO+EA group every day.

Neurological deficit assessment

Neurological deficit score

From day 1 to day 7 after MCAO modeling, neurological deficits were evaluated daily using the Zea Longa 5-point scoring system (0 = no observable deficit; 1 = failure to fully extend the right forepaw; 2 = contralateral circling; 3 = contralateral falling; 4 = no spontaneous locomotion or loss of consciousness).

2,3,5-Triphenyltetrazolium chloride staining

During the intervention period, on the 1st and 7th days respectively, three rats were randomly selected from each group and euthanized under anesthesia for the collection

of brain tissues. 2,3,5-triphenyltetrazolium chloride (TTC) staining was used to stain the meningeal sections, and the stained brain slices of rats in each group were photographed using a digital camera. Image Pro-Plus (version 6.0) software was used to investigate and calculate the infarct size, based on the following formula: percentage of infarction (percentage) = [pale area mass/(pale area mass+nonpale area mass)] × 100%.

Nissl staining

Nissl staining was performed following conventional dewaxing and hydration procedures. Paraffin sections were immersed in tar purple staining solution and then baked at 56 °C for 1 h. Subsequently, the sections were immersed in 0.5% hydrochloric acid ethanol fractionation solution for 4–20 s. Following dehydration, the sections were sealed with neutral gel and stored away from light. A 400× light microscope was used to investigate the morphological and structural alterations in the rat brain.

Immunohistochemistry and immunofluorescence

Immunohistochemistry: On the first day, tissue sections with a thickness of 3 μm were prepared, dewaxed, and rehydrated. Antigen retrieval was performed using heat or enzymatic methods to restore antigen activity. Nonspecific binding sites were blocked with goat serum, followed by incubation with specific primary antibodies targeting the antigen of interest overnight (NLRP3 antibody; GSDMD antibody). On the second day, labeled secondary antibodies were added to bind to the primary antibodies. The antigen-antibody complexes were then visualized using a chromogenic substrate. Finally, the slides were examined under a light microscope.

Immunofluorescence: On the first day, tissue sections with a thickness of 3 μm were fabricated. Subsequently, they underwent fixation, permeabilization and were blocked with a blocking solution to minimize nonspecific binding. Specific primary antibodies were added and incubated overnight to bind to the target antigens (NLRP3 antibody; GSDMD antibody). On the second day, fluorescently labeled secondary antibodies were applied to bind to the primary antibodies. Nuclei were counterstained with DAPI (4',6-diamidino-2-phenylindole), and the samples were mounted with antifade mounting medium for fluorescence preservation. Finally, the samples were observed under a fluorescence microscope to detect the fluorescent signal.

Western blot analysis

Damaged brain tissue (80 g) was homogenized with 200 μL of RIPA lysis buffer (containing protease inhibitor). Total protein was extracted from the brain tissue of each rat. The BCA assay kit was used to calculate the sample protein concentration, and denaturation was performed in a metal bath at 95 °C for 10 min. After sample loading, electrophoresis, membrane transfer, and blocking with 5% skim milk powder for 2 h, the membrane was incubated overnight at 4 °C with primary antibodies against caspase-1, NLRP3, GSDMD, IL-Iβ, IL-18, and microtubulin (1SDS-PAGE 3000). Subsequently, the membranes were washed and incubated with secondary antibodies (sheep antimouse IgG at 1:1000 dilution and sheep antirabbit IgG at 1:1000 dilution). After detection using a hypersensitive electrochemiluminescent kit, the images were obtained using an ECL imaging system. Image Pro Plus software was used to assess the gray value of each target protein/β-tubulin, and the gray value of the bands was used to detect the relative expression intensity of the target protein.

Real-time fluorescent quantitative PCR

RNA was extracted from the brain tissue of each group, and cDNA was synthesized with the reverse transcription kit. The cDNA was used as a template for PCR on a fluorescence quantitative PCR instrument. Primers were synthesized by Guangzhou Ruibo Biological Co., Ltd. (Table 1). Total RNA was extracted using TRIzol reagent, and 1 μg of total RNA was reverse transcribed with the reverse transcription kit. Subsequently, 2 μL of first-strand cDNA solution was used for amplification according to the amplification kit. All experiments were performed for 40 amplification cycles on the Biological System 7500 System according to the manufacturer's instructions. The threshold cycle (Ct) of the target product was normalized to the internal reference β-actin, and the relative expression was calculated using the comparative cycle threshold (ΔΔCt) method.

ELISA

Rat brain tissue was taken, ground, and centrifuged at 4 °C at 3000*g* for 20 min to collect the supernatant. The concentrations of IL-1β and IL-18 in the brain tissue were then determined using an ELISA kit. Briefly, 100 μL of capture antibody was added at 4 °C, the plate was washed three times, and 200 μL of assay diluent was added to the plate, which was blocked at room temperature for 1 h. Then, 100 μL of standard dilutions of IL-1β and IL-18 were added, and the plate was incubated at 37 °C for 1 h. After repeated washing, the substrate was added to each

Table 1 Primers for qPCR target genes

Primer names	Primer sequence (5'–3')	Length of product (bp)
NLRP3	F: GACCTCAACAGACGCTACACC R: CCACATCTTAGTCCTGCCAAT	102
IL-1β	F: CAGACCCCAAAAGATTAAGGATTG R: CTAGCAGGTCGTCATCATCC	263
Caspase-1	F: TGGAAAAGGCACGAGACC R: GGGCAAAACTTGAGGGAAC	256
GSDMD	F: ATGAGAAAAAGAGGACCTTTGAGC R: TCCTCATTGGTTCCATCTGACTTG	142
β-actin	F: GCCATGTACGTAGCCATCCA R: GAACCGCTCATTGCCGATAG	375

well, and the plate was incubated at room temperature for 20 min. Quantitative absorbance was then obtained via ELISA at 450 nm according to the IL-1β and IL-18 protein standards.

Statistical analysis

SPSS 20.0 (IBM Corporation, Armonk, USA) statistical software was used for all data analyses. The experimental results were expressed as mean ± SD ($\bar{x}$ ± SD). For group comparisons, one-way ANOVA was performed. Statistical significance was defined as $P \leq 0.05$.

Results

Electroacupuncture has neuroprotective effects on neurological function in middle cerebral artery occlusion rats

On the first day of the intervention, the neurological function scores and infarct volumes of the MCAO group, MCAO+EA group, and MCAO+MCC950 group were all significantly higher than those of the sham operation group (Figs. 1a and b, $^{\#}P < 0.05$, $^{\#\#\#}P < 0.001$), but there were no differences among them. On the 7th day of the intervention, the neurological function score and cerebral infarction volume were significantly lower in the MCAO+EA group and the MCAO+MCC950 group than in the MCAO group (Figs. 1a and c, $^{\#\#}P < 0.01$, $^{\#\#\#}P < 0.001$). Nissl staining demonstrated the morphology and quantity of neuronal cells in the cerebral cortex on the 1st and 7th days. In contrast to the sham operation group, the Nissl staining area of the striatum in the MCAO group exhibited a significant decrease in Nissl bodies. In comparison with the MCAO group, the Nissl staining area of the striatum in the MCAO+EA group and the MCAO+MCC950 group manifested a significant increase in Nissl bodies (Figs. 1d and e, $^{\#\#\#}P < 0.001$). These results suggest that EA can improve the neurological function score and cerebral infarction volume and has neuroprotective effects similar to those of the MCAO+MCC950 group.

Expression of NLRP3 and GSDMD in the brains of rats with cerebral ischemia-reperfusion after electroacupuncture intervention

Immunohistochemical analysis on day 1 postintervention revealed that the positive cell areas for NLRP3 and GSDMD in the MCAO+EA group and the MCAO+MCC950 group were significantly reduced compared to the MCAO group, with the MCAO group exhibiting the largest positive cell areas. As shown in Figs. 2a and b, a larger positive cell area correlates with higher protein expression, indicating that the MCAO group had the highest expression levels of NLRP3 and GSDMD. On day 7 postintervention, immunohistochemical results demonstrated that the positive cell areas for NLRP3 and GSDMD remained significantly lower in the MCAO+EA and MCAO+MCC950 groups compared to the MCAO group (Figs. 2c and d). The MCAO group again showed the largest positive cell areas, confirming its highest expression levels of NLRP3 and GSDMD. Overall, as illustrated in Fig. 2, both NLRP3 and GSDMD expression levels were significantly lower on day 7 compared to day 1, with a corresponding reduction in positive cell area ($^{***}P < 0.001$, $^{\#}P < 0.05$, $^{\#\#}P < 0.01$, $^{\#\#\#}P < 0.001$, Figs. 2a–d).

In immunofluorescence experiments, NLRP3 and GSDMD were mainly expressed in the cytoplasm and costained with DAPI. Double immunostaining showed the coexistence of both NLRP3 and GSDMD. On the 1st and 7th days, the fluorescence intensity of the MCAO group was significantly higher than that of the Sham group, while the fluorescence intensity of the MCAO+EA group and the MCAO+MCC950 group was significantly lower than that of the MCAO group ($^{***}P < 0.001$, $^{\#\#}P < 0.01$, $^{\#\#\#}P < 0.001$, Figs. 2e, f).

Electroacupuncture can modulate the expression levels of *NLRP3* and *GSDMD* genes, as well as reduce the expression levels of IL-1β and IL-18

The expression levels of *NLRP3* and *GSDMD* genes in the brain tissues of rats with ischemia-reperfusion injury were determined using real-time fluorescence quantitative detection respectively at 1 day and 7 days after intervention. The MCAO group demonstrated significantly increased expression levels of NLRP3 and GSDMD compared with the sham group. The expression levels of NLRP3 and GSDMD in the MCAO+EA group and MCAO+MCC950 group were significantly lower than those in the MCAO group ($^{***}P < 0.001$, $^{\#\#\#}P < 0.001$, Figs. 3a–d).

The expression levels of IL-1β and IL-18 were detected by ELISA. Compared with those in the sham group, the expression levels of IL-1β and IL-18 were increased after 1, 7 days of treatment. They were significantly lower in the MCAO+EA group and the MCAO+MCC950 group than in the MCAO group ($^{***}P < 0.001$, $^{\#\#\#}P < 0.001$, Figs. 3e–h).

Protein expression levels of GSDMD, NLRP3, caspase-1, IL-1β, and IL-18 in brain tissues

The protein expression levels of NLRP3, GSDMD, caspase-1, IL-1β, and IL-18 were significantly greater in the MCAO group than in the sham group. Compared with those in the MCAO group, the protein expression levels of NLRP3, GSDMD, caspase-1, IL-1β, and IL-18 in the MCAO+EA group were significantly decreased at different time points ($^{**}P < 0.01$, $^{***}P < 0.001$, $^{\#}P < 0.05$, $^{\#\#}P < 0.01$, $^{\#\#\#}P < 0.001$, Fig. 4).

Discussion

EA is considered safe for use and administration. Currently, the mechanism of EA in stroke therapy has

Fig. 1

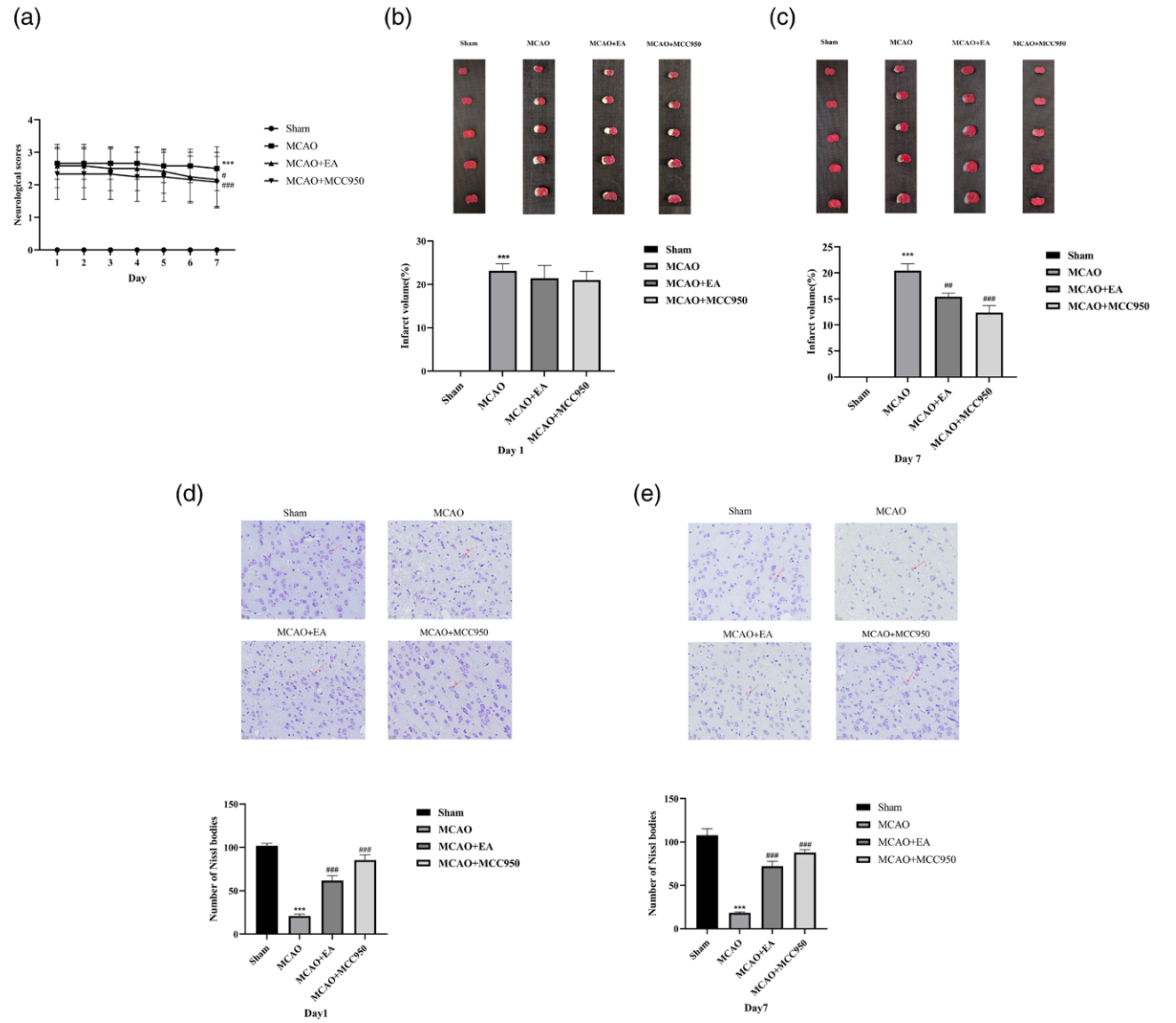

Electroacupuncture therapy significantly enhanced neurological recovery, as evidenced by improved neurological deficit scores and reduced infarct volume following ischemia-reperfusion injury. (a) Cranial nerve function was scored according to the neurological function evaluation table after ischemia-reperfusion in rats. $^{***}P < 0.001$ vs. the sham group, $^{\#}P < 0.05$, $^{\#\#\#}P < 0.001$ vs. the MCAO group ($n = 12$ rats per group); (b and c) TTC maps of cerebral infarction volume on the 1st (b) and 7th (c) days after ischemia-reperfusion [The normal brain tissue assumes a red color (#EFEDD0) whereas the infarcted area takes on a white color (#EFEDD0)]. $^{***}P < 0.001$ vs. the sham group, $^{\#\#}P < 0.01$, $^{\#\#\#}P < 0.001$ vs. the MCAO group (1st the MCAO+EA group and the MCAO+MCC950 group vs. the MCAO group no statistically significant difference). Data were expressed as mean ± SD ($n = 3$ rats per group); (d and e) Nissl staining shows the morphology and number of neuronal cells in the cerebral cortex on days 1 and 7, compared with the sham group, the Nissl-stained area of the striatum in the MCAO group shows a significant reduction in Nissl bodies (red arrow points to the living neuron cell). $^{***}P < 0.001$ vs. the sham group. Compared with the MCAO group, the number of Nissl bodies in the MCAO+EA group and the MCAO+MCC950 group is significantly higher after intervention, and the cell morphology is more complete. $^{\#\#\#}P < 0.001$ vs. the MCAO group. Scale = 20 μm. Data were expressed as mean ± SD ($n = 3$ rats per group). EA, electroacupuncture; MCAO, middle cerebral artery occlusion; TTC, 2,3,5-triphenyltetrazolium chloride.

not been fully elucidated. However, available evidence strongly suggests the efficiency of EA in promoting the rehabilitation of nerve function after stroke [14]. Some of the ways through which it exerts its beneficial effects include, but are not limited to, inhibiting neuronal autophagy and apoptosis, alleviating nerve inflammation, promoting angiogenesis, and stimulating the proliferation and differentiation of endogenous neural stem cells [6,7]. Recent studies suggest that GV20 and GV14 may be transmitted via the following pathways: GV20 stimulates Aβ mechanoreceptors via Piezo2 channels, with signals transmitted through the trigeminal nerve to the nucleus tractus solitarius. GV14 activates Aδ/C nociceptors via TRPV1, relaying through C7 spinal nerves to the spinal

Fig. 2

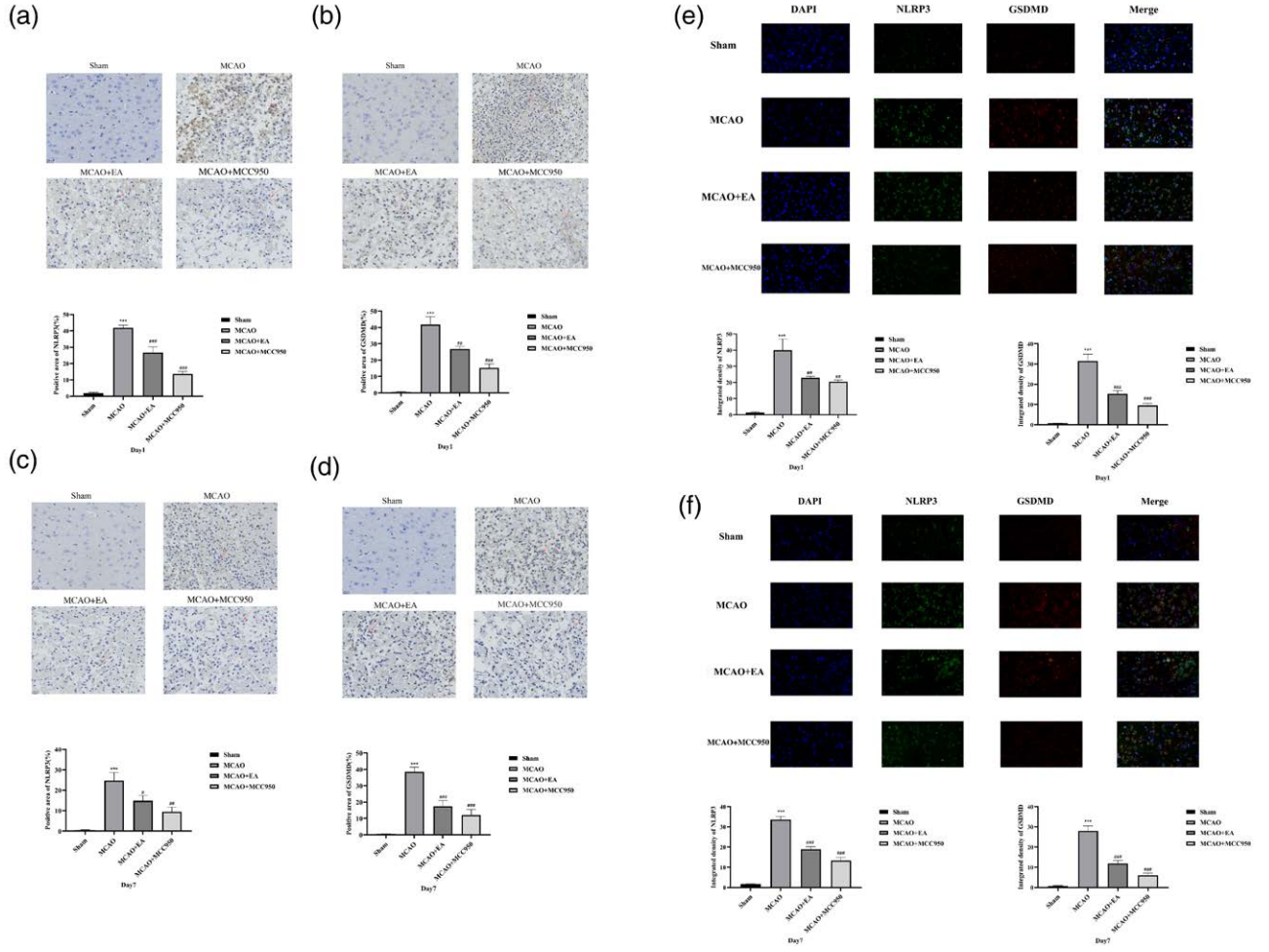

NLRP3/GSDMD expression in the brains of rats with ischemia-reperfusion injury. (a–d) Immunohistochemical analysis was conducted on the 1st and 7th days postelectroacupuncture (EA) intervention to evaluate the expression and localization of NLRP3 (a and c) and GSDMD (b and d) in each group (***$P < 0.001$, #$P < 0.05$, ##$P < 0.01$, and ###$P < 0.001$). Both NLRP3 and GSDMD were predominantly localized in the cytoplasm. The extent of positive cell area correlated with protein expression levels, with red arrows indicating positive cells. Scale bar=20 μm. Data were expressed as mean ± SD ($n = 3$ rats per group). (e) Immunofluorescence staining showed the expression and localization of NLRP3 and GSDMD in each group. NLRP3 and GSDMD were mainly expressed in the cytoplasm and costained with DAPI. Double immunostaining showed the coexistence of NLRP3 and GSDMD (red arrows point to positive cells). (***$P < 0.001$, ##$P < 0.01$, ###$P < 0.001$). Scale bar = 40 μm. Data were expressed as mean ± SD ($n = 3$ rats per group). (f) Immunofluorescence staining showed the expression and localization of NLRP3 and GSDMD in each group. NLRP3 and GSDMD were mainly expressed in the cytoplasm and costained with DAPI. Double immunostaining showed the coexistence of NLRP3 and GSDMD (red arrows point to positive cells). (***$P < 0.001$, ###$P < 0.001$). Scale bar = 40 μm. Data were expressed as mean ± SD ($n = 3$ rats per group).

dorsal horn. Both pathways converge at the ventroposterolateral thalamic nucleus, projecting to the somatosensory cortex via the medial lemniscal pathway, synchronized by theta-gamma crossfrequency coupling [15]. Astrocyte-driven plasticity in laminae II–III involves TNF-α/NF-κB-mediated glutamate-GABA crosstalk [16] and miR-132-KCC2 suppression [17], balancing nociception and proprioception. Frequency-divergent routing directs 2 Hz signals to thalamic μ-opioid receptors, while 100 Hz signals engage parvalbumin interneurons to phase-lock cortical gamma oscillations [18]. Thalamocortical gating via TRN burst/tonic modes and 4 Hz theta rhythms enhance prefrontal-limbic theta-gamma coupling [19], coordinating vagal-adrenal anti-inflammation and BDNF-TrkB-dependent dendritic remodeling, driving functional recovery [20].

Extensive data have confirmed the important role of neuroinflammation in brain injury following ischemia-reperfusion trauma [21]. Therefore, we hypothesize that EA might suppress neuroinflammation in ischemic stroke and facilitate the restoration of neurological function. Studies have shown that microglia are activated after cerebral ischemia, producing large amounts of neurotoxic molecules and proinflammatory cytokines that exacerbate

Fig. 3

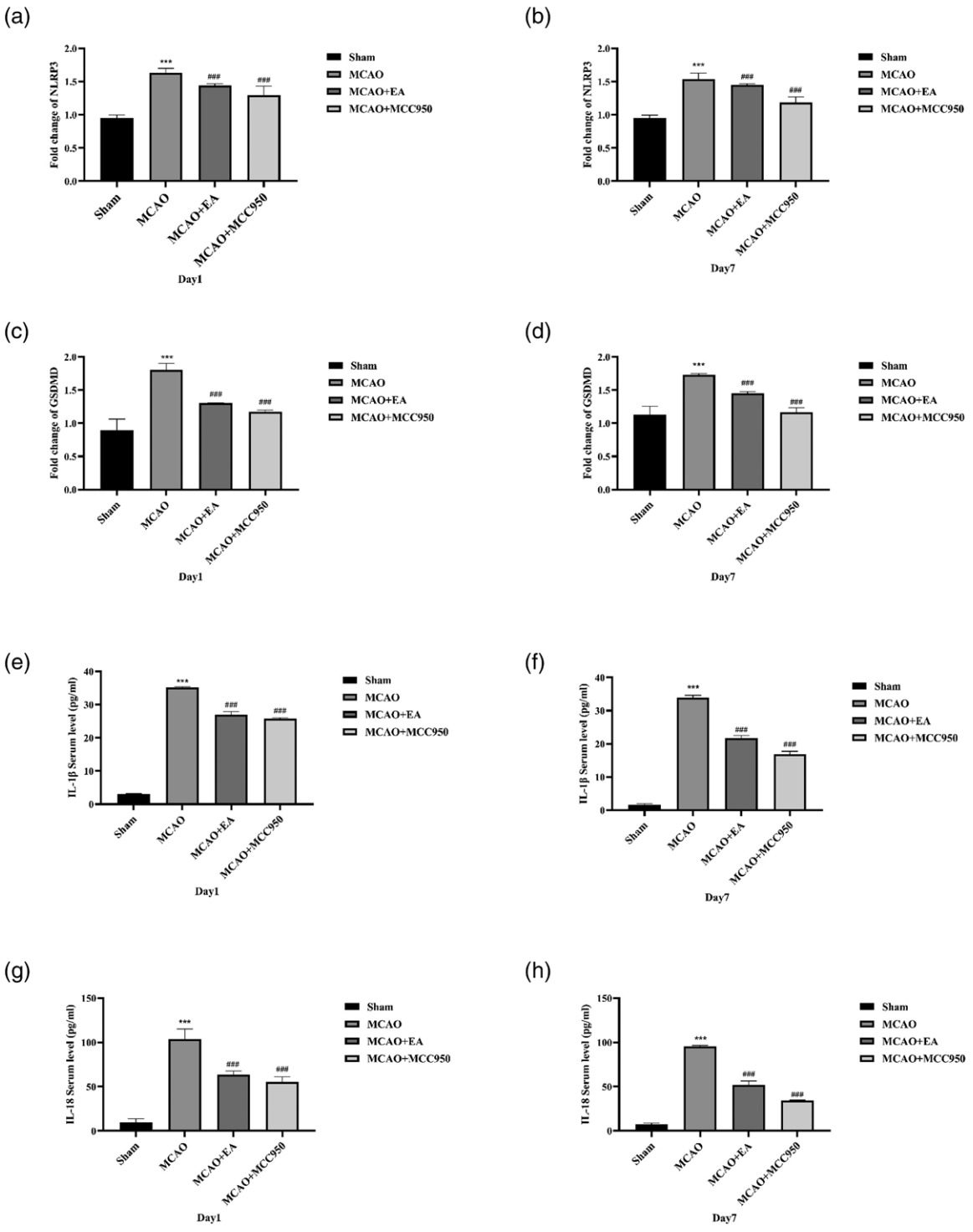

The expression levels of *NLRP3* and *GSDMD* genes as well as IL-1β and IL-18 in rats on the 1st and 7th days after intervention. (a–d) Real-time fluorescence quantitative detection of NLRP3 (a, b) and GSDMD (c, d) gene expression levels in the brain tissue of rats with ischemia-reperfusion injury after 1 day and 7 days of intervention. The MCAO group demonstrated significantly increased expression levels of NLRP3 and GSDMD compared with the sham group. $^{***}P < 0.001$ vs. the sham group. The expression levels of NLRP3 and GSDMD in the MCAO+EA group and MCAO+MCC950 group were significantly lower than those in the MCAO group. $^{###}P < 0.001$ vs. the MCAO group. Data were expressed as mean ± SD ($n = 3$ rats per group). (e–h) IL-1β (e, f) and IL-18 (g, h) expression levels on days 1 and 7, respectively; the expression of IL-1β and IL-18 was significantly lower in the MCAO group compared to the sham group. $^{***}P < 0.001$ vs. the sham group. The MCAO+EA group and MCAO+MCC950 group showed significantly lower expression of IL-1β and IL-18 than the MCAO group. $^{###}P < 0.001$ vs. the MCAO group. Data were expressed as mean ± SD ($n = 3$ rats per group). EA, electroacupuncture; MCAO, middle cerebral artery occlusion.

Fig. 4

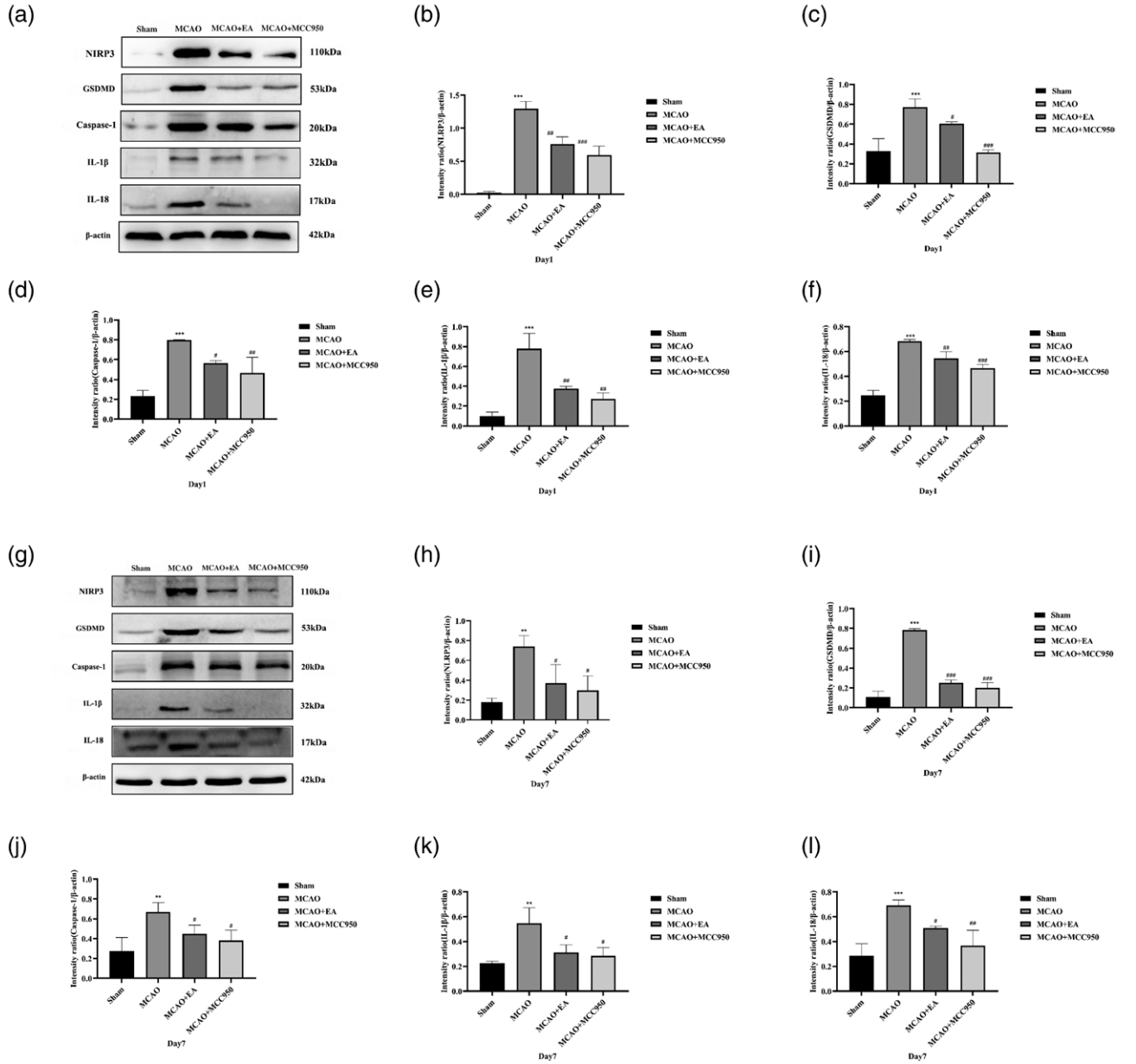

The expression levels of proteins associated with the NLRP3/caspase-1 inflammatory pathway were assessed at 1 day and 7 days postelectroacupuncture treatment. (a–f) On the first day after intervention, the WB experiment showed that the expression levels of NLRP3, GSDMD, caspase-1, IL-1β, and IL-18 were significantly higher in the MCAOl group compared to the sham group. $^{***}P < 0.001$ vs. the sham group. Compared to the MCAO group, the expression levels of NLRP3, GSDMD, caspase-1, IL-1β, and IL-18 were significantly lower in the MCAO+EA group and the MCAO+MCC950 group. $^{\#}P < 0.05$, $^{\#\#}P < 0.01$, $^{\#\#\#}P < 0.001$ vs. the MCAO group. Data were expressed as mean ± SD ($n = 3$ rats per group). (g–l) After 7 days of intervention, the WB experiment showed that the expression levels of NLRP3, GSDMD, caspase-1, IL-1β, and IL-18 were significantly higher in the MCAO group compared to the sham group. $^{**}P < 0.01$, $^{***}P < 0.001$ vs. the sham group. Compared to the MCAO group, the expression levels of NLRP3, GSDMD, caspase-1, IL-1β, and IL-18 were significantly lower in the MCAO+EA group and the MCAO+MCC950 group. $^{\#}P < 0.05$, $^{\#\#}P < 0.01$, $^{\#\#\#}P < 0.001$ vs. the MCAO group. Data were expressed as mean ± SD ($n = 3$ rats per group). EA, electroacupuncture; MCAO, middle cerebral artery occlusion.

brain damage [22]. Considering their prevalence in the central nervous system, NLRP3 inflammatory vesicles are highly concerning [23]. In ischemic brain injury, the NLRP3 inflammasome is important for mediating inflammation [24]. Its essential components are NLRP3, ASC, and caspase-1 [25]. The entire assembly of the NLRP3 inflammasome is activated when it is stimulated by endogenous or external activating irritants [26]. Activated NLRP3 activates caspase-1, which enhances IL-1 and IL-18 biosynthesis and drives inflammatory responses

through various downstream signaling pathways, thereby resulting in neuronal damage [27]. Inhibiting NLRP3 has shown promise in enhancing neurological function following cerebral ischemia [28], making the NLRP3 inflammasome a crucial therapeutic target for ischemic stroke. Previous studies have demonstrated the efficacy of EA in inhibiting neuroinflammation in ischemic stroke and promoting the repair of neurological function. This effect appears to be associated with the EA-induced inhibition of the NLRP3/caspase-1 inflammatory pathway and the subsequent reduction in the expression of pyroptosis-related proteins. In this case, it was hereby hypothesized that the neuroprotective mechanism of EA in MCAO rats might be achieved by inhibiting the NLRP3/caspase-1 inflammatory pathway.

When selecting acupoints, Renzhong (GV26), Neiguan (PC6), Quchi (LI11), Zusanli (ST36), GV14, and GV20 are frequently used as the main acupoints for the treatment of stroke. In this study, GV14 and GV20 acupoints were selected to evaluate the effect of EA treatment on an MCAO rat MCAO and explore its potential mechanism. The adoption of GV14 and GV20 acupoints in this study stems from traditional Chinese medicine theory, which posits that these points belong to the Du meridian and are closely associated with the brain and deemed effective in treating neurological diseases. The GV14 acupoint plays a crucial role in modulating the immune function of the organism. Ischemic stroke can induce inflammatory responses and immune dysfunctions in the organism. EA at GV14 and GV20 synergistically treat stroke through spatiotemporally distinct mechanisms. GV14 activates spinal-sympathetic pathways to enhance splenic macrophage phagocytosis and polarizes microglia to anti-inflammatory M2 phenotypes. Concurrently, it promotes Treg-mediated suppression of Th17-driven IL-6/TNF-α and inhibits neutrophil extracellular traps [29]. Chronic GV14 stimulation enables microglia-neuron metabolic coupling for synaptic repair. GV20 leverages its neurovascular niche via Piezo2-mediated mechanotransduction in perivascular macrophages to trigger trigeminovascular Aδ fiber signals and induce cortical LTP and BDNF-TrkB-dependent axonal sprouting. GV20 also enhances mitochondrial biogenesis and suppresses microglial NLRP3 via noradrenergic β2-AR signaling. Combined, GV20 optimizes neurovascular coupling and glymphatic clearance, while GV14 sustains immunometabolic homeostasis. Their frequency-divergent integration outperforms single-acupoint effects by coupling angiogenesis with oligodendrogenesis, achieving spatiotemporally precise neural repair and anti-inflammatory protection [30,31]. To this end, the GV14 and GV20 acupoints were selected to evaluate the effect of EA treatment on the MCAO rat model to explore its potential mechanism.

Our study showed a statistically significant improvement in neurological function scores after EA treatment compared to those in the MCAO group. The neurological function score is an essential indicator for evaluating brain function impairment, and can visually and accurately reflect the degree of brain damage after cerebral ischemia and recovery after treatment. Furthermore, Nissl bodies are important indicators of nerve function, and the number of Nissl bodies can decrease or even disappear when nerve function is impaired. Our study showed that the number of Nissl bodies was significantly increased in the MCAO+EA group compared to the MCAO group, indicating that EA can promote nerve function recovery. TTC staining of brain sections also showed the same results, with smaller infarct volumes in the MCAO+EA group than in the MCAO group. These results suggest that EA can promote nerve function repair after ischemic stroke. The results of Western blotting revealed an increased expression of NLRP3 and caspase-1 in the MCAO group, which supported our hypothesis. Notably, the expression of NLRP3 and caspase-1 decreased in the MCAO+EA group, and the difference was statistically significant when compared with that in the MCAO group. We hypothesize that EA inhibits the activation of NLRP3 inflammatory vesicles and attenuates the release of the inflammatory mediators IL-1β and IL-18. Overactivation of NLRP3 inflammatory vesicles can trigger a cascade of inflammatory responses, culminating in a relatively newly recognized form of cell death called pyroptosis [32]. Our results indicate that significantly higher NLRP3 expression was shown with more severe nerve damage in the MCAO group compared to the sham group. We used immunohistochemical staining to detect obvious positive cells in the MCAO group. In contrast, the cells in the sham surgery group and the MCAO+EA group did not undergo necrosis, and the number of positive cells was significantly lower than that in the MCAO group. Secondly, we used diaminobenzidine to detect intracellular peroxidase activity in the terminal deoxynucleotidyl transferase dUTP nick-end labeling fluorescence staining, and detected obvious brownish-yellow cells in the MCAO group. In contrast, the cells in the sham and MCAO+EA groups were not necrotic and did not react with the marker, and a significant number of normal blue cells were visible. The increase in the number of normal cells in the EA treatment group suggested that EA treatment can reduce neuroinflammation and promote neuronal cells. EA has been shown to alleviate neuroinflammation by reducing the expression of the NLRP3/caspase-1 inflammasome. According to the results of this study, EA acupuncture at GV14 and GV20 may have a unique mechanism of action on ischemic brain injury. EA treatment can enhance the recovery of neurological function and reduce the inflammatory response. The underlying mechanism may be related to the regulation of NLRP3/caspase-1.

In conclusion, elevated levels of NLRP3 in MCAO rats are an important cause of brain injury, and inhibiting

NLRP3 activation or reducing its level may be a potential therapeutic strategy for treating cerebral ischemic injury.

Acknowledgements

All animal experiments and protocols complied with international animal experimental ethics and requirements, and were approved by the Animal Ethics Committee of Yunnan University of Chinese Medicine (License No. SD-2024-057).

This work was supported by the General Project of Yunnan Applied Basic Research Program (No. 202201AT070214), Yunnan Provincial Science and Technology Department-Applied Basic Research Joint Special Funds of Chinese Medicine (Nos. 202001AZ070001-020 and 202301AZ070001-016) and two types of talent projects in Yunnan Province (No. 202205AD160024). Yunnan Provincial Department of Science and Technology Basic Research Special Project (No. 202201AU070176). Yunnan Provincial Joint Special Project on Basic Research of Traditional Chinese Medicine (No. 202301AZ070001-026).

Every author participated in the designing, conduction and data collection of the study. And contributed to the experimental conduction and results interpretation. Z.W. finished the manuscript writing. Y.X. and J.L. performed data analysis. J.Y., T.S., and S.X. assisted in the experimental conduction. L.X. made revisions to the manuscript. P.P. has edited the manuscript. J.W. approved the final manuscript.

The raw data applied in the study will be available for all qualified researchers without any reservation.

Conflicts of interest

The authors declare that they have no known competing financial interests or personal relationships that could have appeared to influence the work reported in this article.

References

1 Dahl S, Hjalmarsson C, Andersson B. Sex differences in risk factors, treatment, and prognosis in acute stroke. *Womens Health (Lond)* 2020; **16**:1745506520952039.
2 Mo Y, Sun YY, Liu KY. Autophagy and inflammation in ischemic stroke. *Neural Regen Res* 2020; **15**:1388–1396.
3 Najjar S, Pearlman DM, Alper K, Najjar A, Devinsky O. Neuroinflammation and psychiatric illness. *J Neuroinflammation* 2013; **10**:43.
4 Tang B, Li Y, Xu X, Du G, Wang H. Electroacupuncture ameliorates neuronal injury by NLRP3/ASC/Caspase-1 mediated pyroptosis in cerebral ischemia-reperfusion. *Mol Neurobiol* 2024; **61**:2357–2366.
5 Zahid A, Li B, Kombe AJK, Jin T, Tao J. Pharmacological inhibitors of the NLRP3 inflammasome. *Front Immunol* 2019; **10**:2538.
6 Zhu H, Jian Z, Zhong Y, Ye Y, Zhang Y, Hu X, *et al*. Janus Kinase inhibition ameliorates ischemic stroke injury and neuroinflammation through reducing NLRP3 inflammasome activation via JAK2/STAT3 pathway inhibition. *Front Immunol* 2021; **12**:714943.
7 Sha R, Zhang B, Han X, Peng J, Zheng C, Zhang F, Huang X. Electroacupuncture alleviates ischemic brain injury by inhibiting the miR-223/NLRP3 pathway. *Med Sci Monit* 2019; **25**:4723–4733.
8 Wang J, Zhang C, Yang J, *et al*. Effects of near-far acupuncture on neuronal function and expression of apoptosis-related protein Bax/Bcl-2/Cleaved caspase-3 in rats with ischemic stroke. *Acupunct Electrother Res* 2021; **45**:73–86.
9 Longa EZ, Weinstein PR, Carlson S, Cummins R. Reversible middle cerebral artery occlusion without craniectomy in rats. *Stroke* 1989; **20**:84–91.
10 Chi KL, Wen J, Zhang X, Jia CS, Zhang X, Gao F, *et al*. Visual data mining and analysis of literature on electroacupuncture treatment for sequelae of stroke. *Acupunct Res* 2023; **48**:508–514.
11 Yin L, Tang T, Lin Y, Yang M, Liu W, Liang S. Functional connectivity of ipsilateral striatum in rats with ischemic stroke increased by electroacupuncture. *J Integr Neurosci* 2022; **21**:162.
12 Fu LW, Gong YD, Nguyen AT, Guo ZL, Tjen-A-Looi SC, Malik S.s Sympathoinhibitory electroacupuncture (EA) interacts positively with anti-inflammatory EA alleviating blood pressure in hypertensive rats. *Front Cardiovasc Med* 2023; **10**:1140255.
13 Ward R, Li W, Abdul Y, Jackson LD, Dong G, Jamil S, *et al*. NLRP3 inflammasome inhibition with MCC950 improves diabetes-mediated cognitive impairment and vasoneuronal remodeling after ischemia. *Pharmacol Res* 2019; **142**:237–250.
14 Wu R, Ma H, Hu J, Wang D, Wang F, Yu X, *et al*. Electroacupuncture stimulation to modulate neural oscillations in promoting neurological rehabilitation. *Brain Res* 2024; **1822**:148642.
15 Cheng CY, Lin JG, Tang NY, Kao ST, Hsieh CL. Electroacupuncture-like stimulation at the Baihui (GV20) and Dazhui (GV14) acupoints protects rats against subacute-phase cerebral ischemia-reperfusion injuries by reducing S100B-mediated neurotoxicity. *PLoS One* 2014; **9**:e91426.
16 Lu H, Ai L, Zhang B. TNF-α induces AQP4 overexpression in astrocytes through the NF-κB pathway causing cellular edema and apoptosis. *Biosci Rep* 2022; **42**:BSR20212224.
17 Yau JO, Chaichim C, Power JM, McNally GP. The roles of basolateral amygdala parvalbumin neurons in fear learning. *J Neurosci* 2021; **41**:9223–9234.
18 Song J, Sun J, Moss J, Wen Z, Sun GJ, Hsu D, *et al*. Parvalbumin interneurons mediate neuronal circuitry-neurogenesis coupling in the adult hippocampus. *Nat Neurosci* 2013; **16**:1728–1730.
19 Krugliakova E, Volk C, Jaramillo V, Sousouri G, Huber R. Changes in cross-frequency coupling following closed-loop auditory stimulation in non-rapid eye movement sleep. *Sci Rep* 2020; **10**:10628.
20 Lin B, Zhang L, Yin X, Chen X, Ruan C, Wu T, *et al*. Modulation of entorhinal cortex-hippocampus connectivity and recognition memory following electroacupuncture on 3×Tg-AD model: evidence from multimodal MRI and electrophysiological recordings. *Front Neurosci* 2022; **16**:968767.
21 Cnop M, Toivonen S, Igoillo-Esteve M, Salpea P. Endoplasmic reticulum stress and eIF2α phosphorylation: the Achilles heel of pancreatic β cells. *Mol Metab* 2017; **6**:1024–1039.
22 Pirzada RH, Javaid N, Choi S. The roles of the NLRP3 inflammasome in neurodegenerative and metabolic diseases and in relevant advanced therapeutic interventions. *Genes (Basel)* 2020; **11**:131.
23 Krainer J, Siebenhandl S, Weinhäusel A. Systemic autoinflammatory diseases. *J Autoimmun* 2020; **109**:102421.
24 Chauhan D, Vande Walle L, Lamkanfi M. Therapeutic modulation of inflammasome pathways. *Immunol Rev* 2020; **297**:123–138.
25 Meyers AK, Zhu X. The NLRP3 inflammasome: metabolic regulation and contribution to inflammaging. *Cells* 2020; **9**:1808.
26 Bai B, Yang Y, Wang Q, Li M, Tian C, Liu Y, *et al*. NLRP3 inflammasome in endothelial dysfunction. *Cell Death Dis* 2020; **11**:776.
27 Samir P, Malireddi RKS, Kanneganti TD. The PANoptosome: a deadly protein complex driving pyroptosis, apoptosis, and necroptosis (PANoptosis). *Front Cell Infect Microbiol* 2020; **10**:238.
28 Sapkota A, Choi JW. Oleanolic acid provides neuroprotection against ischemic stroke through the inhibition of microglial activation and NLRP3 inflammasome activation. *Biomol Ther (Seoul)* 2022; **30**:55–63.
29 Yen CM, Hsieh CL, Lin YW. Electroacupuncture reduces chronic fibromyalgia pain through attenuation of transient receptor potential vanilloid 1 signaling pathway in mouse brains. *Iran J Basic Med Sci* 2020; **23**:894–900.
30 Zhao Y, Zheng Q, Hong Y, Gao Y, Hu J, Lang M, *et al*. β2-Microglobulin coaggregates with Aβ and contributes to amyloid pathology and cognitive deficits in Alzheimer's disease model mice. *Nat Neurosci* 2023; **26**:1170–1184.
31 Kong X, Liu Z, Zhang R, Xie F'an, Liang R, Zhang Y, *et al*. JMJD2D stabilises and cooperates with HBx protein to promote HBV transcription and replication. *JHEP Rep* 2023; **5**:100849.
32 Gou X, Xu D, Li F, Hou K, Fang W, Li Y. Pyroptosis in stroke-new insights into disease mechanisms and therapeutic strategies. *J Physiol Biochem* 2021; **77**:511–529.